Morphology and Hemodynamics in Isolated Common Iliac Artery Aneurysms Impacts Proximal Aortic Remodeling

SUPPLEMENTAL MATERIAL

Louis P Parker, MEng;[1,2] Janet Powell, MD PhD;[3] Lachlan J Kelsey, BEng;[1,2] Brendon Lim, BEng;[1,2] ; Ray Ashleigh, MD;[4] Maarit Venermo, MD PhD;[5] Igor Koncar, MD;[6] Paul E Norman, DS;[1,7] and Barry J Doyle, PhD.[1,2,8,9]

1. Vascular Engineering Laboratory, Harry Perkins Institute of Medical Research, Perth, Australia.

2. School of Mechanical and Chemical Engineering, The University of Western Australia, Perth, Australia.

3. Vascular Surgery Research Group, Imperial College London, London, UK.

4. University Hospital of South Manchester, Manchester, UK.

5. Division of Vascular Surgery, Helsinki University Central Hospital, Helsinki, Finland.

6. Clinic for Vascular and Endovascular Surgery, Belgrade, Serbia.

7. Medical School, The University of Western Australia, Perth, Australia.

8. Australian Research Council Centre for Personalised Therapeutics Technologies, Australia.

9. BHF Centre for Cardiovascular Science, The University of Edinburgh, Edinburgh, UK.

Sources of Patients in the Isolated CIAA Cohort

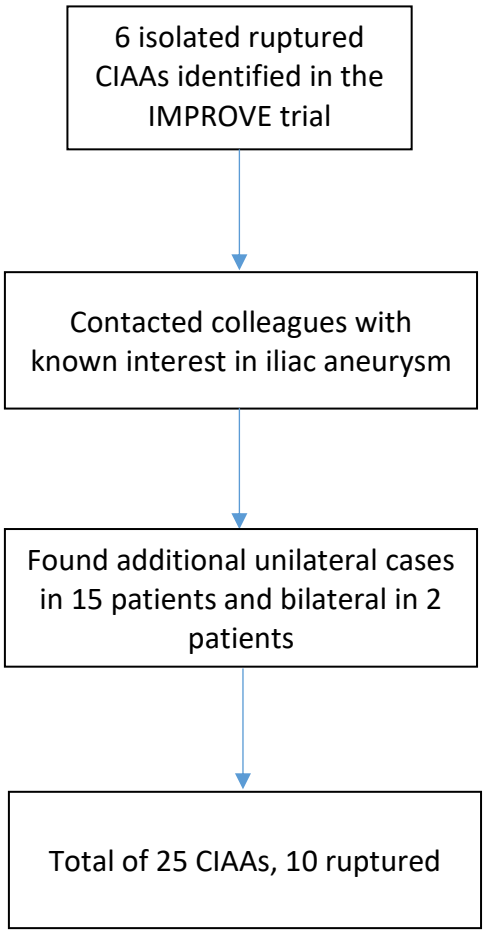


Figure I. Cohort diagram for the isolated CIAA group analysed with CFD.

Reconstruction and Measurement Repeatability for the Isolated CIAA Cohort

Table I. Columns 2 and 3 shows the results of the reconstruction repeatability study. Columns 4-11 show the repeatability of the morphological measurements made. Measurements 1-3 were completed by the primary analyst whilst 4-6 were reconstructed by three separate analysts. Error (ε) is the difference from the mean of the three measurements made.

Measurement	CIAA Recon. Volume (mm^3)	ε (%)	Bifurcation Angle (°)	ε (%)	CIAA Diam. (mm)	ε (%)	Aortic Tortuosity	ε (%)	CIAA Tortuosity	ε (%)
1	293,988	0.03	49.3	0.06	25.6	0.35	0.099	0.44	0.220	0.00
2	284,408	3.29	49.2	0.18	25.5	0.66	0.099	1.05	0.220	0.05
3	303,810	3.31	49.3	0.12	26.0	1.01	0.097	1.49	0.220	0.05
Mean	294,069		49.3		25.7		0.101		0.211	
Std. dev.	9,701		0.1		0.2		0.004		0.014	
4	305,486	2.18	49.3	0.41	26.1	0.87	0.101	1.07	0.220	0.33
5	311,266	0.32	49.3	0.36	25.7	0.57	0.099	1.24	0.221	0.24
6	320,088	2.50	48.7	0.78	25.8	0.30	0.100	0.17	0.222	0.57
Mean	312,280		49.1		25.8		0.100		0.221	
Std. dev.	7,354		0.3		0.2		0.001		0.001	

Isolated CIAA Cohort Simulations

Meshing

CFD relies of the subdivision of the fluid domain into multiple cells (mesh), in which the Navier-Stokes and continuity equations for fluid flow can then be solved. The quality of the mesh influences computational time and accuracy of results. We used an established mesh convergence approach[1] to determine the accuracy of our simulations and assigned areas of high velocity gradients to receive a higher density of cells (e.g. the aortic bifurcation). We used polyhedral cells throughout the fluid domain due to their improved accuracy and reduced computational time and then used prism-layer cells to accurately capture the steep velocity gradient at the boundary of the vessel wall. The thickness of this prism layer t (Eqn. 1) was specified as the distance from the vessel wall to the Hagen-Poiseuille free-stream velocity (half the maximum velocity) and relies on the local vessel radius R.[2, 3]

$$t = \left(1 - \frac{1}{\sqrt{2}}\right) R \qquad \text{Eqn. 1}$$

The prism layer stretching parameter S (Eqn. 2) determines the elongation of the prism layer cells moving away from the vessel wall and allows thinner cells closer to the wall to capture the steep velocity gradient that develops, where n is the total number of prism layers. We have implemented this strategy in our previous simulations. [2, 3]

$$\mathrm{S} = 2^{\left(\frac{1}{n-1}\right)} \qquad \text{Eqn. 2}$$

Mesh Convergence Study

In order to calculate the grid convergence index (GCI) (Roache 1999) the relative error between the results produced from the finest mesh and the medium density mesh must be compared.

$$\varepsilon = \frac{f_2 - f_1}{f_1}$$ Eqn. 3

Where: f = physical parameter observed (f_1 is the result from the finest mesh)

Table II. Meshing parameters applied in the mesh convergence study.

Mesh	Surface Size (mm)	Number of Prism Layers	Polyhedral Cell Density
Coarse	3	3	0.5
Medium	3	6	1
Fine	3	12	

The order of convergence, *p*, must then also be calculated using the grid refinement ratio, *r*.

$$p = \frac{ln\left(\frac{f_3 - f_2}{f_2 - f_1}\right)}{ln(r)}$$ Eqn. 4

These results can then be substituted in to the GCI formula.

$$GCI = \frac{|\varepsilon|}{(r^p - 1)}$$ Eqn. 5

Where: ε = the relative error

Table III. Results of the mesh convergence study.

Location	Physical Parameter	GCI
Aortic Bifurcation	Max WSS	0.7277%
	Mean WSS	0.3374%
Left External Iliac Artery	Velocity	0.0063%
Right External Iliac Artery	Velocity	0.0062%

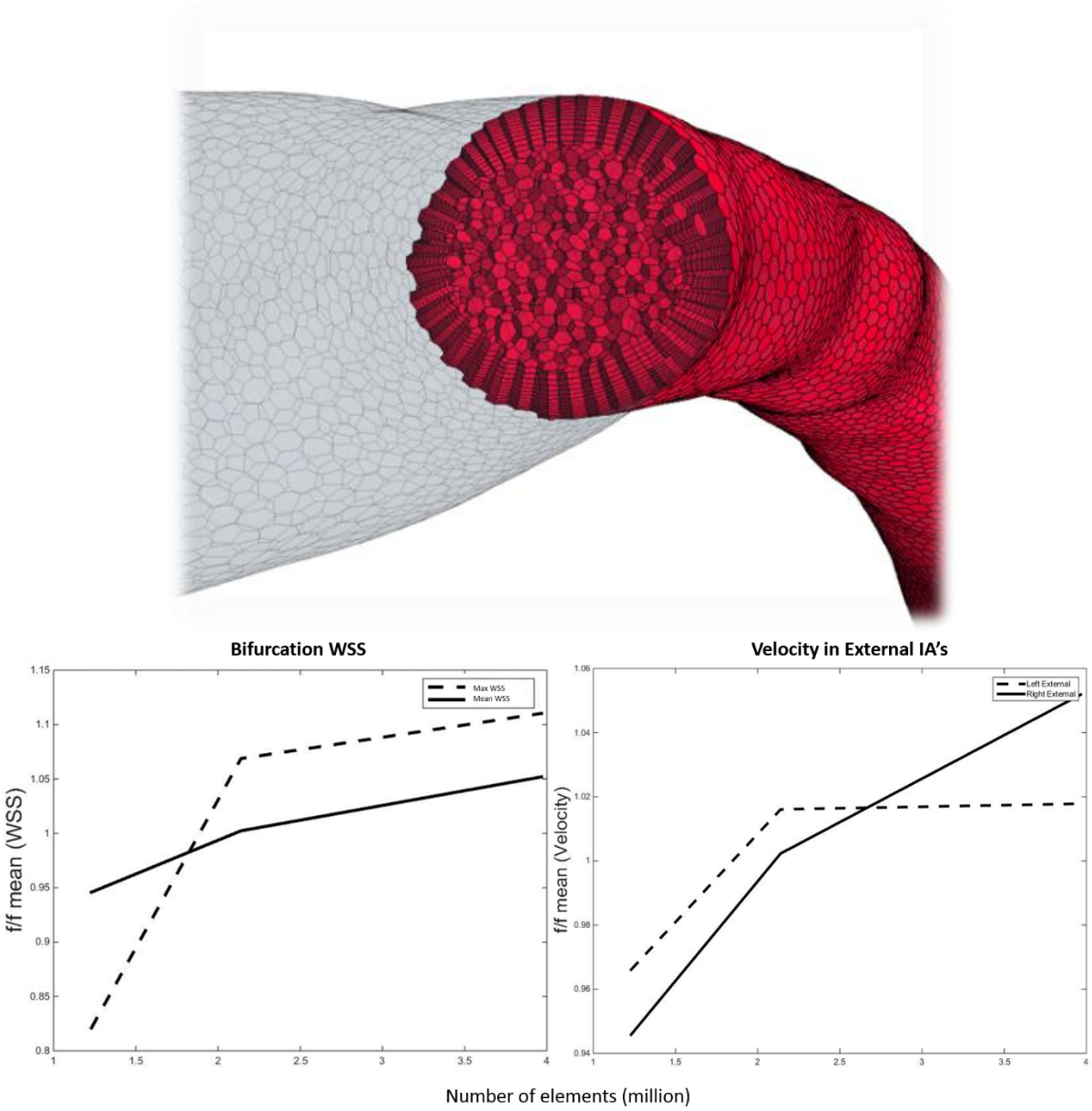


Figure II. (Top) Cross-section of the mesh in the CIA showing the polyhedral core surrounded by prism layer cells near the vessel wall. The high density cells at the surface are prism layer cells used to capture high velocity gradients. (Bottom) Convergence of WSS at the bifurcation surface (left) as well as in the external iliac arteries (right).

Inlet and Outlet Extensions

We added extensions to the inlets and outlets to establish fully developed laminar flow before entering the model and to ensure that the outlet boundary conditions did not affect the upstream

hemodynamics. The inlet length L was calculated using a previous method (Eqn. 6)[4] where a is arterial radius, α is the Womersley number (a dimensionless parameter ranging from 15-20 for the aorta) and Re is the Reynolds number.

$$L = a \times \frac{Re}{\alpha^2} \qquad \text{Eqn .6}$$

We calculated the expected Reynolds number at systole and determined the required inlet length to be 100 mm. We then created outlet lengths 10 times the outlet diameter, as this has been shown to be a sufficient length to remove the effects of an open boundary on the model.[5]

Hemodynamic Metrics

WSS is a measure of the friction force of the blood flow adjacent to the arterial wall. The prevailing conditions are of greater physiological significance than any instantaneous or peak measure and so the TAWSS was recorded for each case. Oscillatory shear index (OSI) quantifies the fluctuation in blood velocity direction and magnitude throughout the cardiac cycle.[6] Endothelial Cell Activation Potential (ECAP) was recently proposed[7] to indicate 'thrombogenic susceptibility' and is the ratio: OSI/TAWSS. Although highly oscillatory flow and low shear stresses are likely to result in thrombus deposition in CIAAs, the term ECAP is misleading as it infers the action of an endothelial layer, not present in many aneurysms. To avoid confusion the ratio is referred to as Low and Oscillatory Shear (LOS) in this study and we also acknowledge that LOS will promote dilation through disruption to steady, laminar flow. WSS is defined by Eqn. 7 where μ is the dynamic viscosity and $\frac{du}{dy}$ is the velocity gradient. TAWSS is defined by Eqn. 8 where T is the period of the cardiac cycle and $\overrightarrow{WSS}$ is the WSS vector.

$$WSS = \mu \cdot \frac{du}{dy} \qquad \text{Eqn. 7}$$

$$TAWSS = \frac{1}{T}\left|\int_0^T \overrightarrow{WSS}\, dt\right| \qquad \text{Eqn. 8}$$

$$OSI = 0.5 \times \left(1 - \frac{\left|\int_0^T \overrightarrow{WSS}\, dt\right|}{\int_0^T \left|\overrightarrow{WSS}\right| dt}\right) \qquad \text{Eqn. 9}$$

$$LOS = \frac{OSI}{TAWSS} \qquad \text{Eqn. 10}$$

Inlet Boundary Condition Sensitivity Analysis

A sensitivity analysis was carried out on the inlet flow assumption by simulating one case of CIAA with 90%, 95%, 105%, 110%, 115% and 120% of the massflow. It was important to test the effect of this assumption as aortic flow is likely to vary greatly from case-to-case particularly with the prevalence of hypertension in patients with aneurysmal disease. A clear linear relationship was seen between the inlet massflow applied and the TAWSS conditions with no significant change in TAWSS surface patterns (see Figure III).

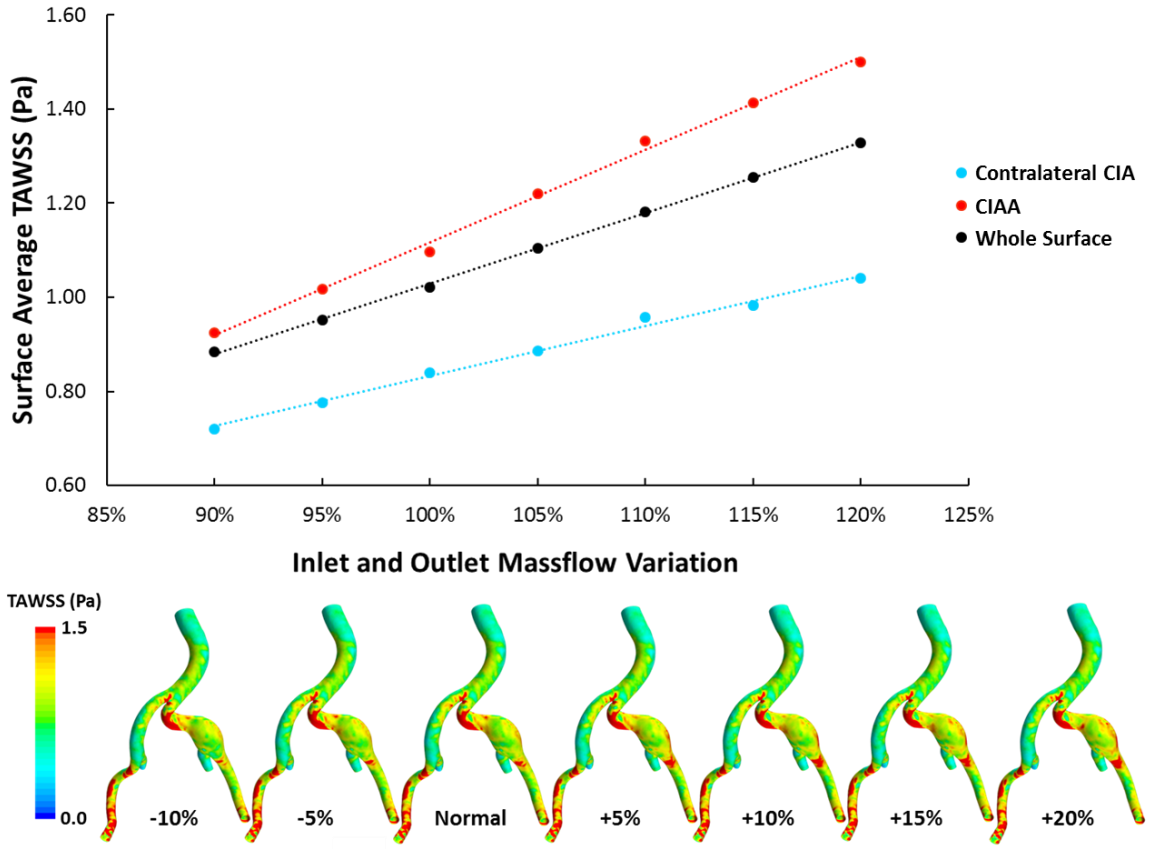


Figure III. (Top) TAWSS is linearly associated with inlet massflow rate with data shown for the contralateral CIA, CIAA and whole model surface. (Bottom) Surface plots of TAWSS with the maximum value scaled according to the change in whole surface TAWSS (maximum of 1.5 Pa for the normal scenario) showing no significant changes in TAWSS patterns with varying inlet flow.

Analysis of a Non-Newtonian Viscosity Model and 3-Element Windkessel Outlets on Surface Results for the CIAA Cohort

The assumption of a Newtonian fluid model for the CIAA cohort is a simplification of the actual viscosity properties of blood. At high shear rates the viscosity of blood increases. To test the effect of this assumption on our results a CIAA simulation was run using the more sophisticated Carreau-Yasuda fluid model to account for this effect.[8] A slight decrease in TAWSS was observed in the abdominal aorta and CIAs with the introduction of this assumption though there was no significant change to OSI. The combined metric of LOS is then very similar. These observations are confirmed quantitatively in Figure IV particularly for our primary regions of interest; the CIA aneurysm and abdominal aorta.

It is common in smaller cohort CFD studies to apply a 3-element Windkessel model to the outlets to simulate the distal arterial bed. A flow split was applied to the CIAA cohort simulations as a simplification. The effect of this simplification was observed by applying a 3-element Windkessel model to one of the CIAA cohort cases. Visually, the simulations were very similar for TAWSS, OSI and LOS. These results are then confirmed quantitatively in Figure V.

The negligible effect of these assumptions on our primary metric of interest, LOS justify the simplifications made, particularly in a relatively large cohort CFD study.

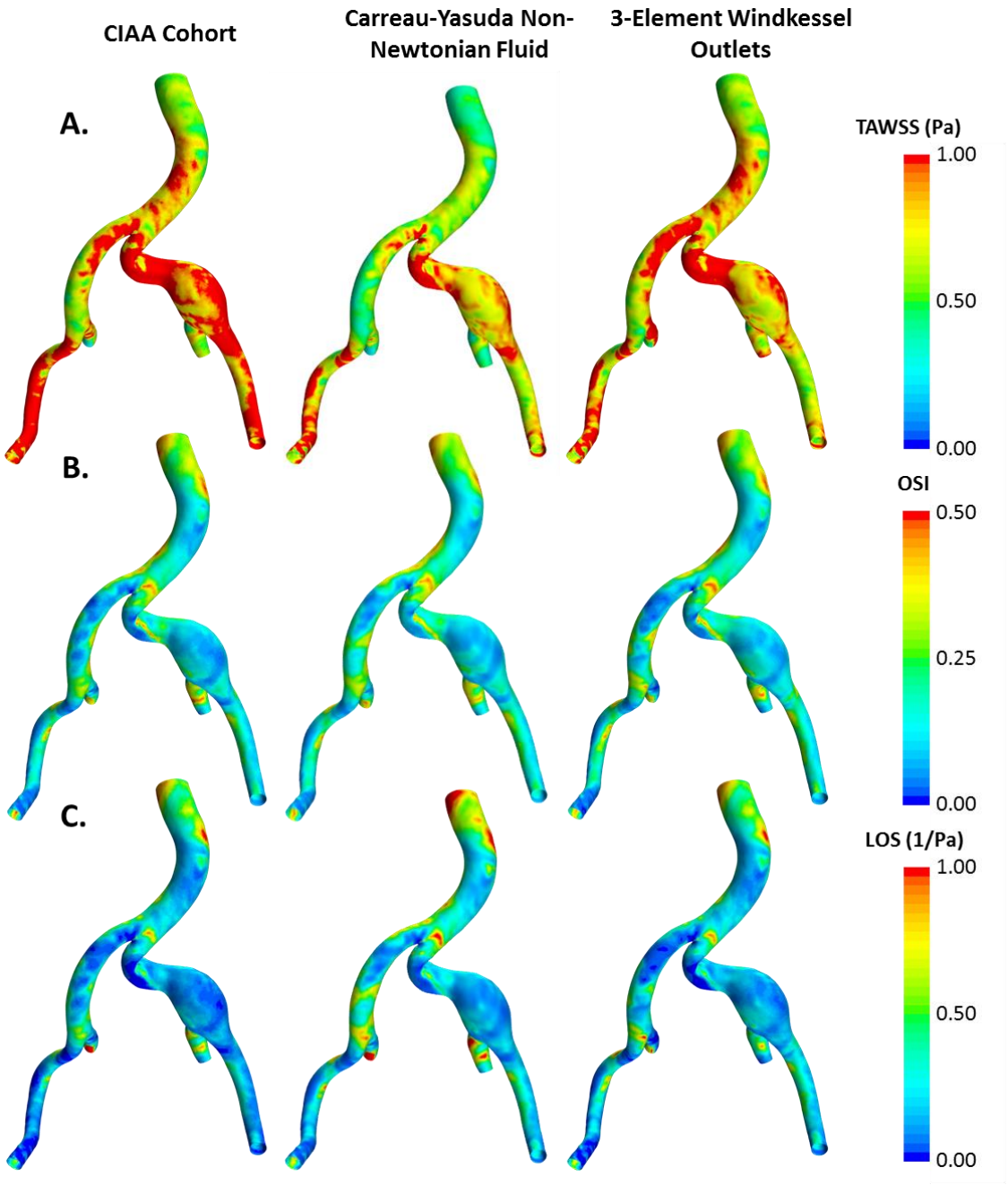


Figure IV. A. The TAWSS results under the standard simulation parameters used for the CIAA cohort (left column), with a non-Newtonian Carreau-Yasuda model (center column) and with 3-element Windkessel outlets (right column). **B.** The OSI results under these three regimes. **C.** The LOS results under these three regimes.

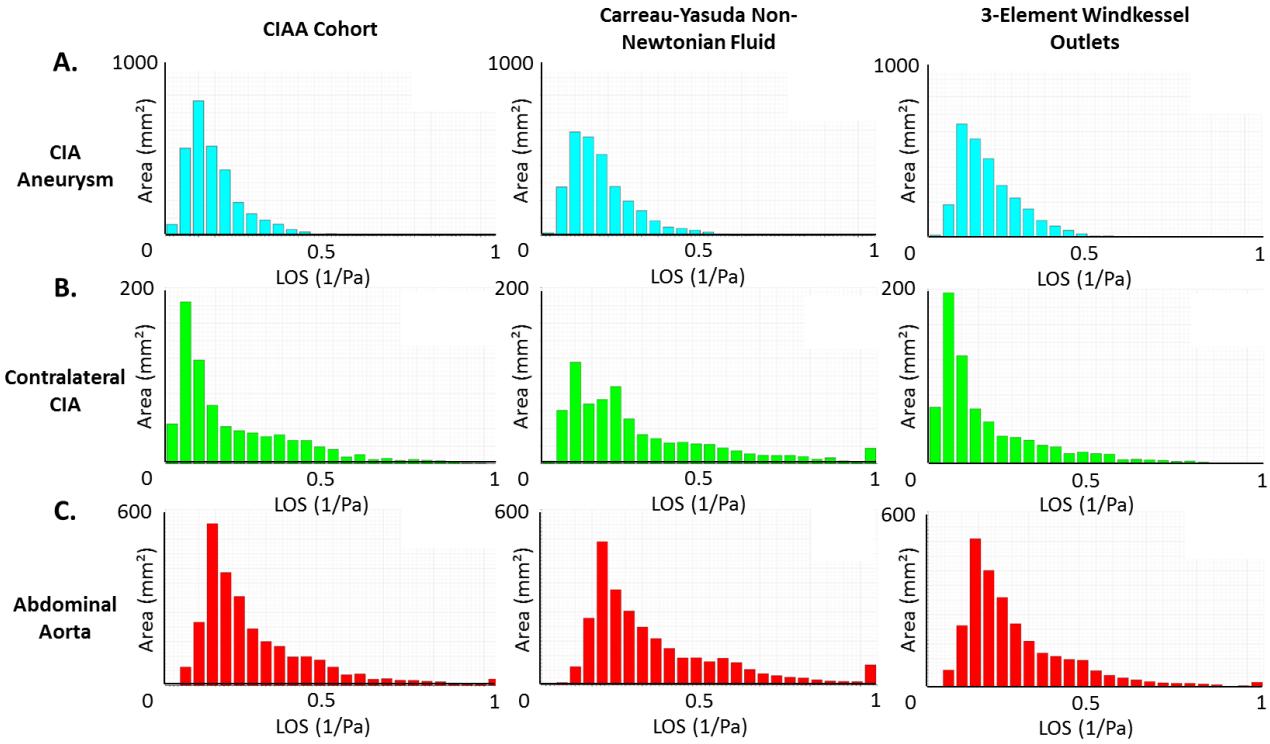


Figure V. A. CIAA, **B**. contralateral CIA and **C.** abdominal aorta surface LOS conditions across the three models.

Sources of Patients in the Validation Cohort

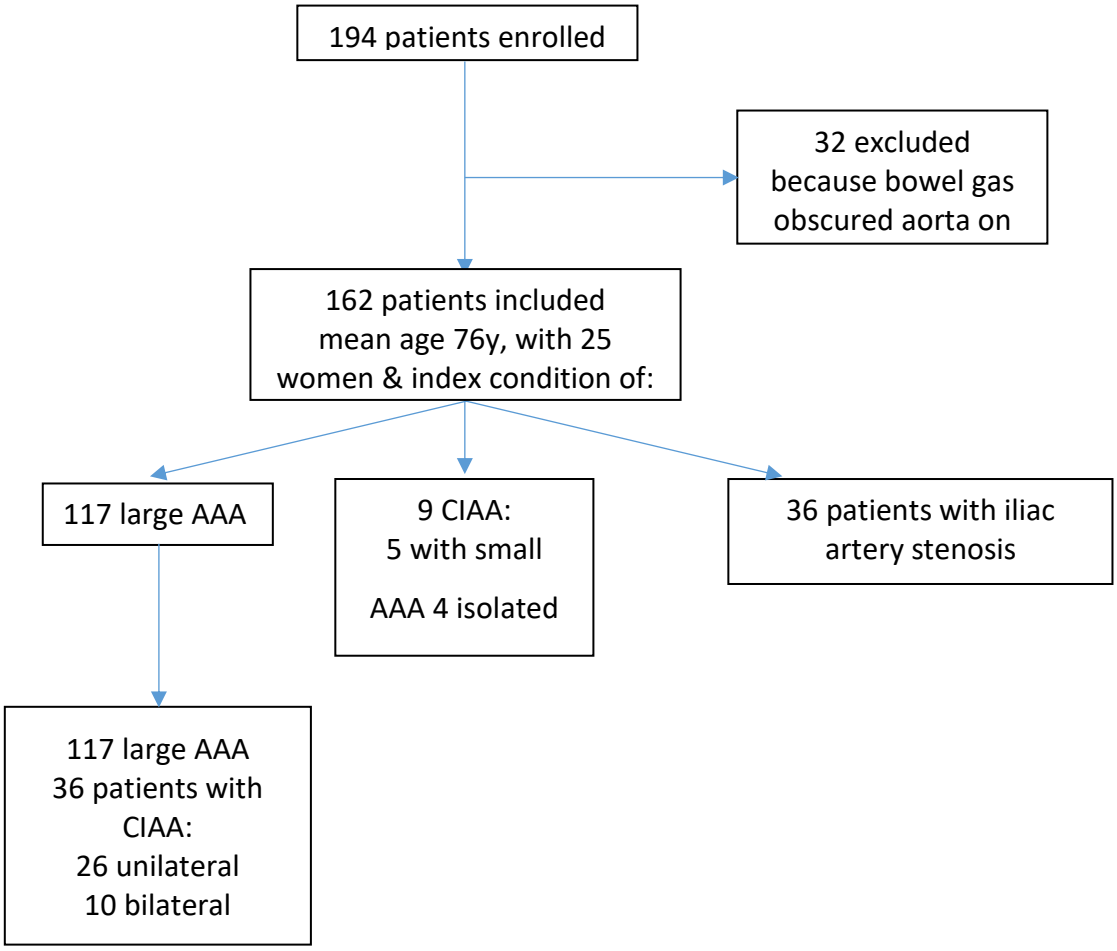


Figure VI. A two single clinician study of consecutive patients enrolled in a study comparing CTA and duplex ultrasonography for planning endovascular intervention, January 2008 to December 2009. The threshold for diagnosing an incidental CIAA was an external (outer-outer) diameter 25 mm.

Characteristics of the Validation Cohort

Table IV. The validation cohort of endovascular intervention patients.

		Left CIA	Right CIA
CIAA present, n	-	30	25
External aortoiliac angle, n (%):			
<90°	-	55 (34)	15 (9)
90°-120°	-	63 (39)	49 (30)
>120°	-	44 (27)	98 (61)
Mean (SD) CIA diameter (mm):			
Deflection to the left (n=86)	21.9 (11.4)	-	-
Deflection to the right (n=25)	23.6 (10.4)	-	-
No significant deflection (n=51)	19.9 (14.2)	-	-
Aortic deflection towards aneurysm in 35 unilateral cases of CIAA, n (%):			
	29 (83)	-	-

* For cohort, mean diameter + 2SD is 25 mm, 10 patients had bilateral CIAAs.

† In one case, no tortuosity measurement was available for both CIAs.

In Silico Hypothetical Series Hemodynamic Plots

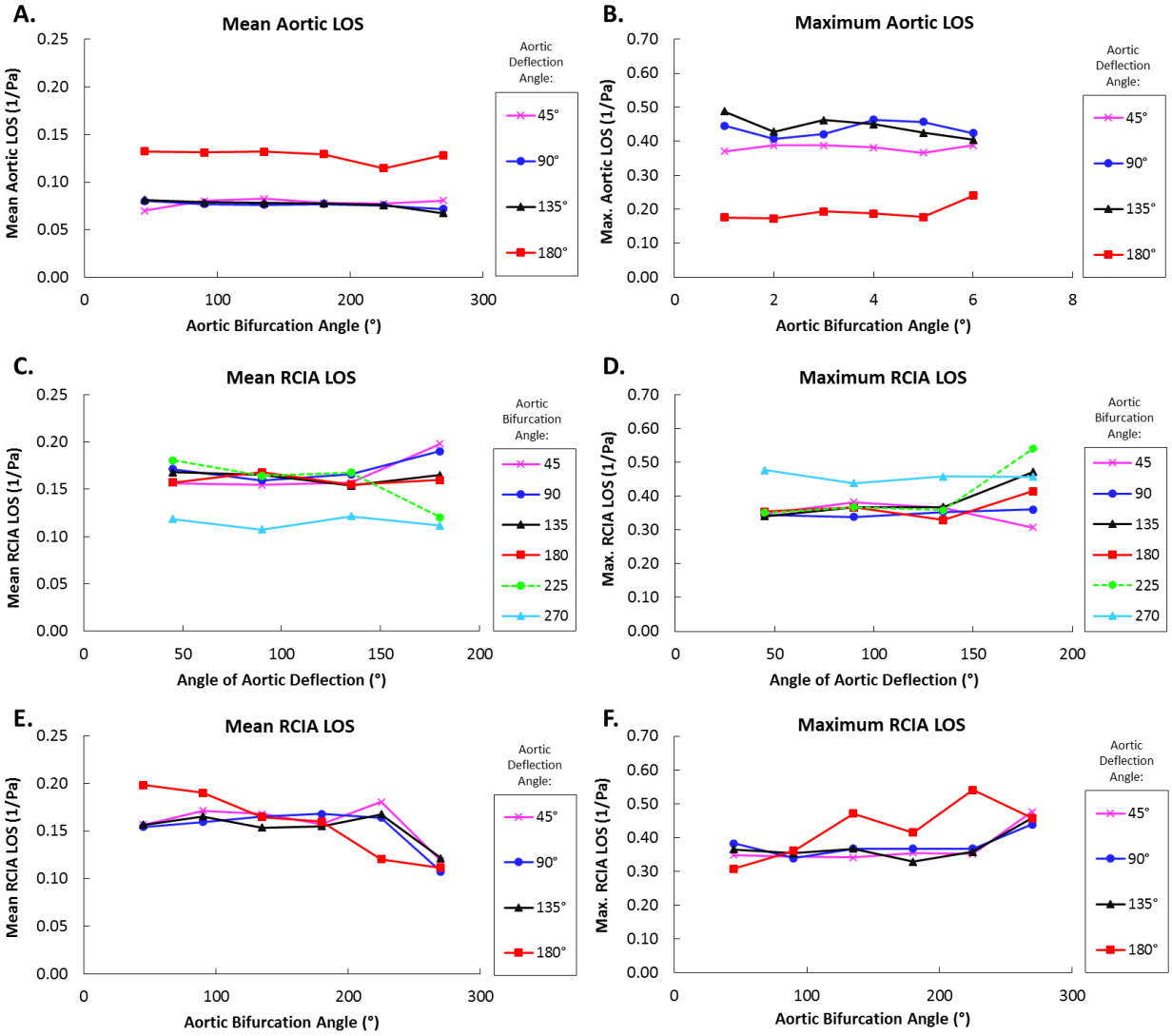


Figure VII. A. The mean LOS in the abdominal aorta as bifurcation angle widens. **B.** The maximum LOS in the abdominal aorta as bifurcation angle widens. **C.** The mean LOS in the RCIA as the angle of aortic deflection is reduced. **D.** The maximum LOS in the RCIA as the angle of aortic deflection is reduced. **E.** The mean LOS in the RCIA as bifurcation angle widens. **F.** The maximum LOS in the RCIA as bifurcation angle widens.

Validation Cohort Morphological Parameter Measurement

Table V. The parameters recorded in the validation cohort.

Parameter	Definition	Notes
Aortic diameter	All external	Includes any ILT
Common iliac artery diameter	Maximum external diameter measured at least 5 mm distal to the bifurcation	Includes any ILT
Tortuosity	Centreline distance from aortic bifurcation point to internal/external iliac bifurcation divided by the linear distance between these two points	Defined as a tortuous artery when this ratio was ≥1.25
External aortoiliac angle	Angle between aorta and first discontinuity in the common iliac artery	3 categories only because of high inter-observer variability (inter-observer repeatability 22**º**) <90 º, 90-120 º and >120 º
Aortic curvature to right (R), left (L) or none (N)	This was based on the intersection of lines from the midpoint of the infra-renal aneurysm neck (or 5 mm below the most distal renal artery for those without AAA) to the centre of the aorta/aneurysm and the line from the aortic bifurcation point to the centre of the aorta/aneurysm.	Curvature was attributed when the acute angle between these lines was 150º or less.

Bifurcation Angle Grades Assigned to the Validation Cohort

The aortic bifurcation angle was not available from the cohort assessed for endovascular intervention, however the external aortoiliac angles were measured (see Figure 2 in main text). Aortic bifurcation angles were then assigned a grade ranging from 1 to 5 based on the combined left and right aortoiliac angles.

Table VI. The bifurcation angles assigned to the validation cohort.

Bifurcation Angle Grade	**Aortoiliac Angles Observed (°)**	**Resulting Bifurcation Angle Range (°)**	**n (%)**
1	<90, <90	180-360	4 (2)
2	<90, 90-120	150-270	23 (14)
3	90-120, 90-120	120-180	57 (35)
4	90-120, >120	60-150	50 (31)
5	>120, >120	0-120	28 (17)

Association Between Bifurcation Angle and CIA Maximum Diameter in the Validation Cohort

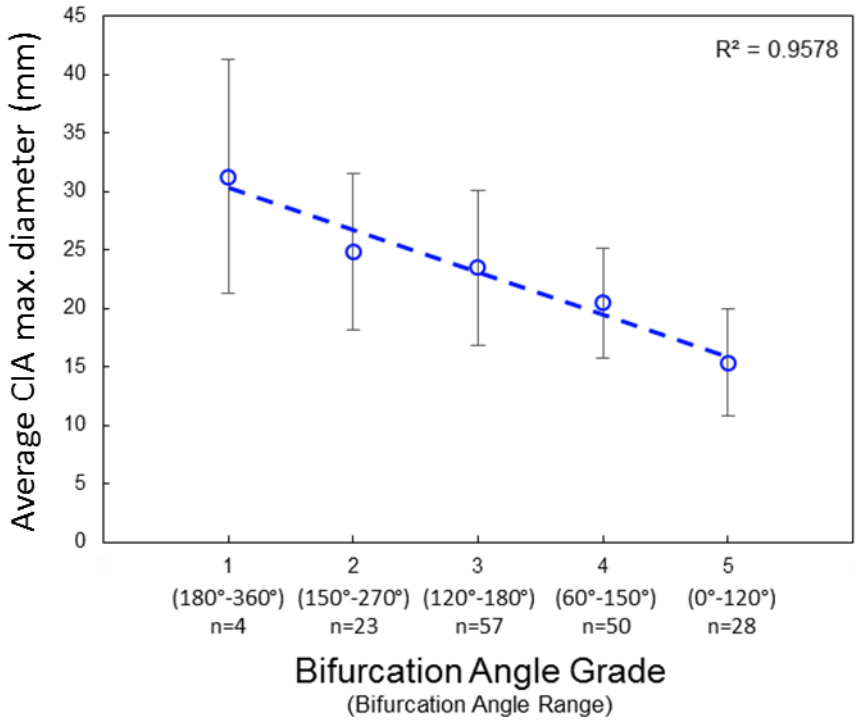


Figure VIII. The average maximum CIA diameter for each bifurcation grade as bifurcation angle narrows in the validation cohort. Bifurcation angle has been assigned a grade from 1-5 based on the measured external aortoiliac angles, with 5 indicating the most acute bifurcation angle.

Surface LOS Values in the *In Silico* Hypothetical Series with Varying Bifurcation Angle

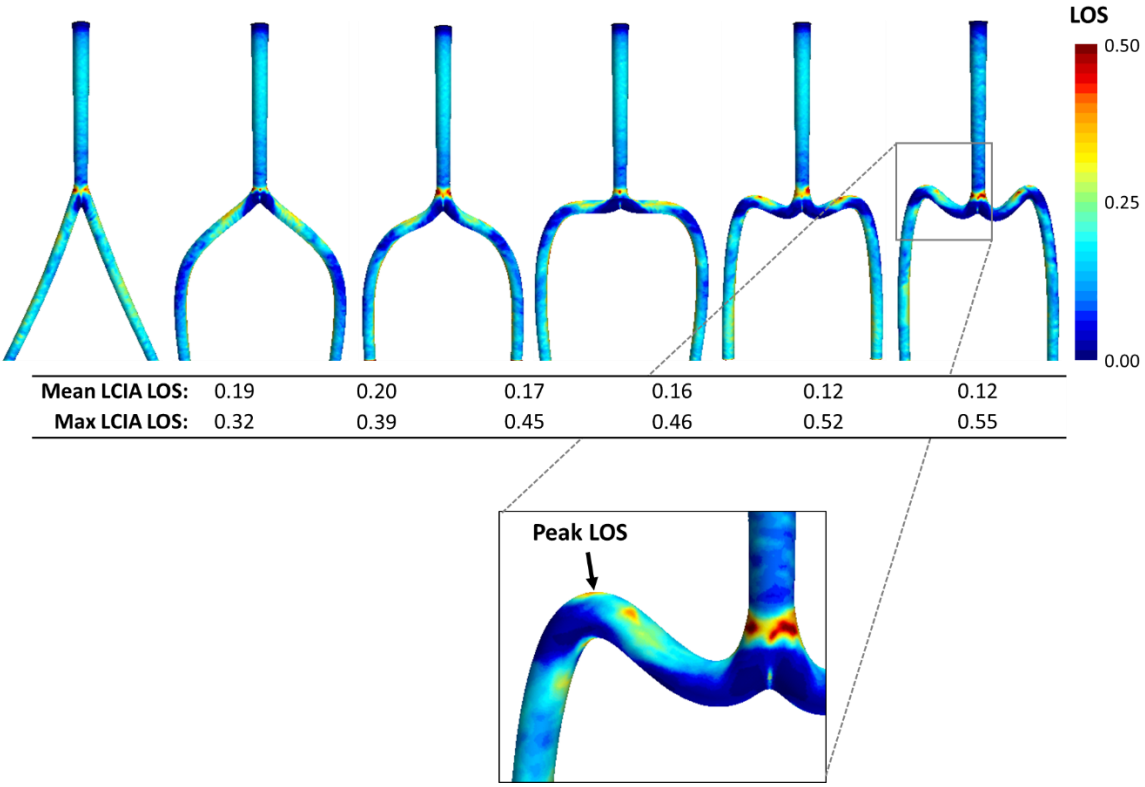


Figure IX. The surface LOS values for the *in silico* hypothetical series with straight aortas and varying bifurcation angles. The magnification shows the uneven distribution of LOS in the CIA as bifurcation angle widens leading to a high peak LOS but decreased surface average LOS.

References

1. Roache PJ. Perspective: A method for uniform reporting of grid refinement studies. *Journal of Fluids Engineering*. 1994;116:405-413
2. Kelsey LJ, Miller K, Norman PE, Powell JT, Doyle BJ. The influence of downstream branching arteries on upstream haemodynamics. *J Biomech*. 2016;49:3090-3096
3. Kelsey LJ, Powell JT, Norman PE, Miller K, Doyle BJ. A comparison of hemodynamic metrics and intraluminal thrombus burden in a common iliac artery aneurysm. *Int J Numer Method Biomed Eng*. 2016;Epub ahead of print:e2821
4. Wood NB. Aspects of fluid dynamics applied to the larger arteries. *J Theor Biol*. 1999;199:137-161
5. Hardman D, Doyle BJ, Semple SI, Richards JM, Newby DE, Easson WJ, Hoskins PR. On the prediction of monocyte deposition in abdominal aortic aneurysms using computational fluid dynamics. *Proc Inst Mech Eng H*. 2013;227:1114-1124
6. Ku DN, Giddens DP, Zarins CK, Glagov S. Pulsatile flow and atherosclerosis in the human carotid bifurcation. Positive correlation between plaque location and low oscillating shear stress. *Arteriosclerosis*. 1985;5:293-302
7. Di Achille P, Tellides G, Figueroa CA, Humphrey JD. A haemodynamic predictor of intraluminal thrombus formation in abdominal aortic aneurysms. *Proc. R. Soc.* 2014;470:1-22
8. Robertson AM, Sequeira A, Owens RG. Rheological models for blood. In: Formaggia L, Quarteroni A, Veneziani A, eds. *Cardiovascular mathematics: Modeling and simulation of the circulatory system*. Milano: Springer Milan; 2009:211-241.